

Ionic nitriding of austenitic and ferritic steel with the aid of a high aperture Hall current accelerator

B. B. Straumal^{1,2}, N. F. Vershinin³, M. Friesel⁴, T. V. Ishenko²,
S. A. Polyakov¹, W. Gust²

¹Institute of Solid State Physics, Russian Academy of Sciences, RU-142432 Chernogolovka,
Russia

²Institut für Metallkunde, Seestr. 92, D-70174 Stuttgart, Germany

³SONG Ltd., RU-142432 Chernogolovka, Russia

⁴SIMS Laboratory, Chalmers University of Technology, S-41296 Gothenburg, Sweden

Keywords: Hall current accelerator; Nitriding; Ion implantation; Steel

Abstract. Ionic implantation technologies play an important role for the surface modification of materials. Recently, a novel Hall current accelerator has been developed. The accelerator has a large aperture of 1400 mm and a power up to 10 kW. High ionic currents up to 1 mA/cm² permit to use the source both for ion implantation and for ionic cleaning of substrates. Various gases can be used for both purposes: argon, nitrogen, oxygen, etc. The current-voltage characteristics for nitrogen at various pressures are presented. The ionic nitriding of austenitic stainless steel and ferritic low-carbon steel has been studied. The influence of ionic current, energy of ions and implantation time are determined. The depth profiles measured with the aid of secondary-ion mass spectroscopy are presented. The hardness after ionic nitriding is characterized, the mechanism of the irradiation-enhanced nitrogen penetration in the austenitic stainless steel is discussed.

Introduction

The nitriding of steels is widely used in metallurgy. In addition to the traditional methods, the ionic nitriding becomes more and more important. The ionic implantation methods traditionally used in the semiconductor technology permit to form alloyed layers buried rather deep in the material (several microns or even tens of microns) due to the high ballistic penetration depth of ions having an energy of several hundreds of keV [1]. However, this method does not fit the requirements of metallurgical applications due to the low ionic flux (below 1-3 $\mu\text{A}/\text{cm}^2$). The low intensity of ionic beams does not permit to produce metallurgically significant concentrations of an implanted element in a reasonable time. A lower energy of ions is used (20-100 keV) in the plasma immersion ionic implantation method (PIII). The lower ballistic depth (about 100 nm) is compensated by a higher ionic flux (about 1 mA/cm²) and additional heating of the substrate (usually to 350-400°C) [2, 3]. PIII permits to produce the alloyed zone of 2 to 10 μm thickness. Recently the method of low-energy high-current ionic implantation (LEHCII) was developed [4, 5]. In this method the energy of ions is below 1 keV (ballistic penetration depth about 5 nm [7]) but the ionic flux is very high, reaching several mA/cm². Particularly, the Kaufman broad beam ionic sources are used for this purpose [2, 5]. LEHCII permits to alloy with nitrogen the surface layers of steels, having a thickness of a few μm even without additional heating [6]. Recently, a high-power large-aperture Hall current accelerator was developed [7, 8]. Hall current accelerators have several important advantages in comparison with Kaufman sources [9-11]. Particularly, the developed Hall current accelerator has a high aperture (1400 mm scalable up to 3000 mm in our case), high power (up to 10 kW), and is more robust and simple in exploitation. It is easy to combine the Hall current accelerator with existing technologies for deposition of coatings. It can be used not only for ionic

cleaning [7, 8] but also for ionic implantation. Various gases can be used for both purposes: argon, nitrogen, oxygen, etc. The aim of this work is to understand the process of nitrogen penetration by low-energy high-current ionic nitriding of austenitic and ferritic steels with the aid of a Hall current accelerator.

Experimental

Hall current accelerator described elsewhere [7, 8] has a form of elongated loop with vertical aperture of 1400 mm and horizontal aperture of 55 mm. The nitrogen implantation into austenitic stainless steel 12X18H9T and low carbon ferritic steel VSt-3-kp (Russian standard GOST 5632) was studied at discharge voltage $U = 900$ V, discharge current $I = 3$ A (ion flux density i about 1 mA/cm^2) during 30, 60 and 90 min. No additional heating of the samples was used. The composition of the steels was controlled by the spark spectral analysis according GOST 22536.13 "Carbon steel and cast iron. Methods of spectral analysis". The carbon content was measured coulombometrically according GOST 22536.1. The 12X18H9T steel contains (in wt. %) 0.11 C, 17.0 Cr, 8.8 Ni, 0.35 Ti, 0.28 Mo, 0.55 Si, 0.35 Mn, Fe (matrix). The VSt-3-kp steel contains 0.19 C, 0.12 Cr, 0.05 Si, 0.30 Mn. Samples having dimensions 20×15 mm were cut from the rolled steel strip of thickness 2 mm, ground and polished. After degreasing in ethanol and distilled water, the samples were mounted at the distance of 10 cm from the Hall current accelerator.

The distribution of C, N, Fe, Cr and Ni in the samples after nitrogen ionic implantation was determined using secondary ion mass spectroscopy (SIMS). An *ims 3f* secondary ion mass spectrometer (Cameca, France) has been used for in-depth analyses of the films and substrates. O_2^+ ions accelerated with energy 12.5 kV were used as primary ions. The primary ion current I_p ranged from 250 to 1800 nA. The primary ion beam was rastered over a square area $250 \times 250 \text{ }\mu\text{m}$. The secondary ions, accelerated by 4.5 kV, were collected from a square area $100 \times 100 \text{ }\mu\text{m}$ in the middle of the rastered area. The energy band pass filter for the secondary ions was 50 eV, centered at the maximum energy of the secondary ions. The distributions of C, N, Ti, Fe, Cr and Ni were studied by profiling isotopes $^{12}\text{C}^-$, $^{14}\text{N}^-$, $^{24}\text{C}_2^-$, $^{28}\text{CO}^-$, $^{26}\text{CN}^-$, $^{56}\text{Fe}^+$, $^{52}\text{Cr}^+$ and $^{60}\text{Ni}^+$ respectively. The $^{26}\text{CN}^-/^{24}\text{C}_2^-$ ratio was used for the estimation of nitrogen concentration by depth profiling due to the very low intensity of $^{14}\text{N}^-$ line. The depth of the sputtered craters was measured with a *Talysurf 10* instrument (Rank Taylor Hobson, UK). Each crater was measured several times in the central region of the crater. The deviation in the average depth ranged from 2 to 11%. The microhardness of the nitrided samples was measured at various loads (from 0.1 to 0.85 N) with the aid of *PMT* instrument (LOMO, Russia).

Results and discussion

In Fig. 1 the voltage-current characteristics for nitrogen discharge are shown for various nitrogen pressures p . It can be seen that at p below 30 mPa the slow increase of discharge current I proceeds with increasing discharge voltage U . At $p = 49$ mPa the voltage-current characteristic differs drastically from those at low p . The high discharge current of about 6 A can be reached already at 2 keV. In Fig. 2 the dependence of microhardness on the load is shown for the untreated stainless steel substrate and after nitriding. The indentation depth changes from $14 \text{ }\mu\text{m}$ at 0.1 N (90 min) to $50 \text{ }\mu\text{m}$ at 0.8 N. Therefore, at high loads the thickness of nitrided layer is negligible in comparison with indentation depth, and the hardness of the bulk material is measured (about 3.2 GPa in all three curves). The hardness of untreated material is nearly independent of the load. The implantation of nitrogen increases the surface hardness of the material. After 30 min the hardness at loads below 0.3 N is higher than that of untreated sample. With increasing duration of ionic nitriding the surface hardness increases as well. After 90 min the hardness at 0.1 N is almost two

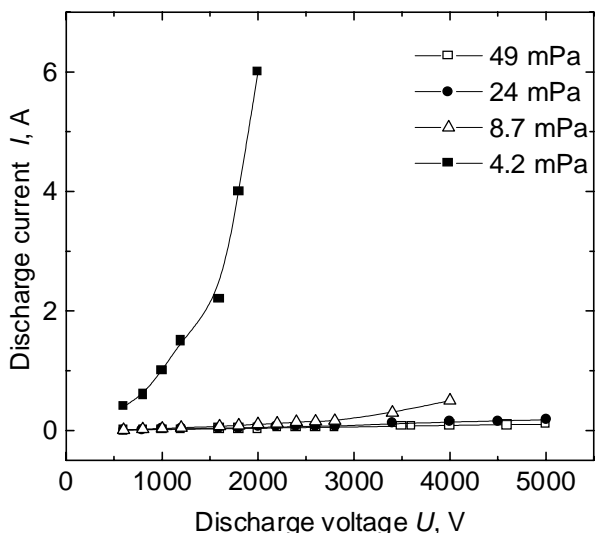


Fig. 1. Current-voltage characteristic for nitrogen at various pressures

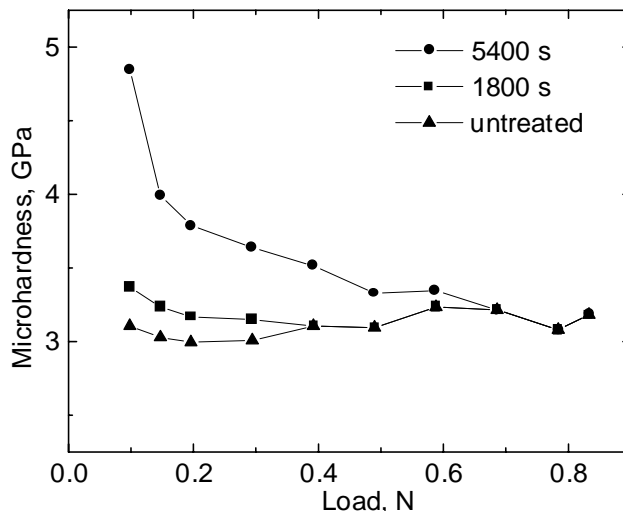


Fig. 2. Dependence of microhardness on applied load for stainless steel nitrided at $U = 900$ V and $i = 1$ mA/cm² after various implantation times

times higher than that of the untreated material. The thickness of the nitrided layer increased as well, namely the hardness drops down to the bulk value only at load of 0.6 N. The depth of the nitrided layer could be roughly estimated from the curves shown in the Fig. 1. It can be supposed that the measured hardness reaches the bulk value if the thickness of the hardened layer is less than 0.1 of indentation depth. This estimation gives about 3 μ m for the thickness of the hardened layer.

In the Fig. 3 SIMS depth profiles are given for 30, 90 and 120 min treatments. The rough quantification of SIMS depth profiles made using the layer of Fe₄N phase on the 99.9% Fe shows that the maximal concentration of nitrogen is at least a few to 10 at. % N. The depth of nitrided layer increases with increasing implantation time t . The penetration depth for low carbon steel is slightly higher than that for stainless steel. Therefore, the estimation given above delivers overestimated

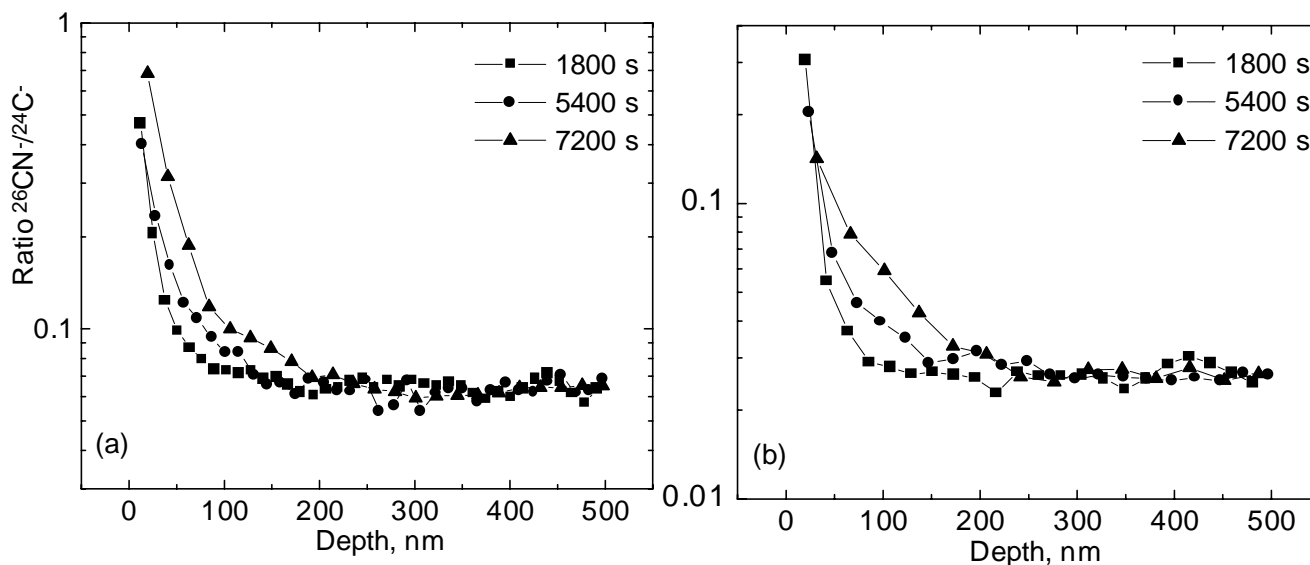


Fig. 3. SIMS depth profiles for low-carbon (a) and stainless steel (b) nitrided at $U = 900$ V and $i = 1$ mA/cm² after various implantation times.

values for the thickness of hardened layer. On the other hand, the microhardness values are underestimated even by load of 0.1 N. Therefore, the measurement of nanohardness with lower loads are needed for the correct estimation of the surface hardness. The thickness of the nitrided layer obtained in our experiments without additional heating of the samples is only slightly lower than that of layer obtained in comparable conditions (700 keV, 2 mA/cm², 60 min) by heating up to 280 °C [6].

The thickness of penetration layer is two orders of magnitude higher than the ballistic penetration depth for 900 V and about 2 to 4 orders of magnitude higher than the length of conventional bulk diffusion of nitrogen. Therefore, the paradoxically deep penetration of nitrogen cannot be explained neither by ballistic penetration nor by conventional diffusion. The mechanism of this process seems unusual and needs to be clarified. In particular, the role of very high ionic current and possible non-equilibrium phase transformations have to be studied.

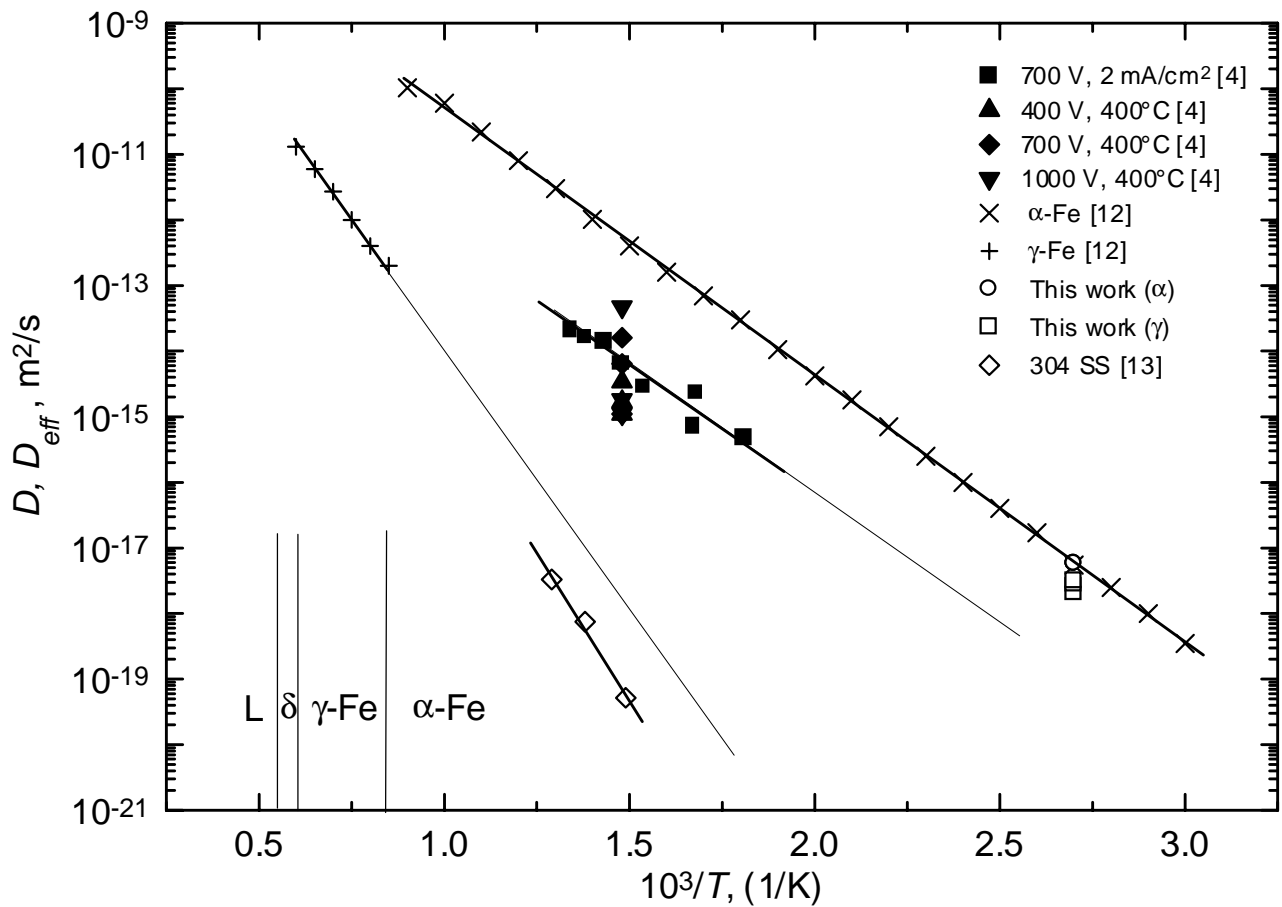


Fig. 3. The temperature dependence (Arrhenius plot) for the diffusion coefficient D of nitrogen in α -Fe [12], γ -Fe [12] and stainless steel [13] and for the effective diffusion coefficient estimated as $D_{eff} = L^2/t$ for the low-energy high-current ionic implantation of nitrogen. The values of D_{eff} were calculated using the data [4] for the influence of U and i at 400°C and for the temperature influence at $U = 700$ eV and $i = 2$ mA/cm². The data for the influence of the implantation time on D_{eff} in stainless steel (γ) and low-carbon steel (α) into non-heated substrate were obtained in this work.

The data for the bulk diffusion coefficient (D) of nitrogen and the effective diffusion coefficient $D_{eff} = L^2/t$ (t being the implantation duration and L the penetration depth) during ion implantation are plotted in Fig. 3. The data for the bulk diffusion in α -Fe and γ -Fe are taken from the literature

[12]. The extrapolation of the data for γ -Fe into α -Fe area is shown by thin line. The experimental points for bulk diffusion of nitrogen in AISI 316 austenitic stainless steel (SS) measured in the temperature range 400-500°C [13] are lower than the D data for γ -Fe extrapolated into the α -Fe area. The activation energy Q for the diffusion of N in 316 SS is only slightly higher than Q for the bulk diffusion of N in γ -Fe. The low-voltage high-current nitrogen ion implantation into AISI 304 stainless steel was studied recently [4]. It has been shown that the penetration depth increases with increasing substrate temperature T , ion energy U and ionic current density i . We plotted these data in Fig. 3 as D_{eff} for comparison with the bulk diffusion of N in Fe and stainless steel [12, 13]. The D_{eff} values obtained as the result of low-energy high-current ion implantation of N are about 3 to 5 orders of magnitude higher than the extrapolated values for the bulk diffusion in γ -Fe and about 4 to 6 orders of magnitude higher than the D values for diffusion of N in AISI 304 stainless steel. On the other hand, D_{eff} is about one order of magnitude lower than D for the diffusion of N in α -Fe. The activation energy for D_{eff} at $U = 700$ V and $i = 2$ mA/cm² in the temperature range 200-600°C is lower than the activation energy for the bulk diffusion of N in γ -Fe and 304 SS; it is close to the value for the diffusion of N in α -Fe. At $T = 400$ °C and $i = 2$ mA/cm², the D_{eff} value for the ion implantation at $U = 700$ V is higher than $D_{eff}(U = 400$ V) and lower than $D_{eff}(U = 1000$ V). At $T = 400$ °C and $U = 700$ V, the D_{eff} value for $i = 2$ mA/cm² is higher than $D_{eff}(i = 1$ mA/cm²) and lower than $D_{eff}(i = 3$ mA/cm²).

The high penetration depth of N in austenitic stainless steel cannot be explained by ballistic penetration of the nitrogen ions it is only about 10 nm since for the energy studied (700-1000 eV) [6]. Due to the high density of the ion flux, low-energy ion implantation is a very non-equilibrium process. Particularly, during the nitrogen implantation into austenitic stainless steel, a layer of supersaturated solid solution is formed called *expanded austenite* with a N content exceeding the equilibrium solubility of N in γ -Fe [2]. Under certain conditions, the resulting mechanical stresses can lead to the formation of an amorphous phase in the implanted zone [14–16]. The data on the microstructural investigation of the low-energy high-current N-implanted layer in the austenitic stainless steel reveal the existence of amorphous and nanostructured layers in the implanted zone [17]. The step-like form of the penetration profiles of N after low-energy high-current implantation reveals also the existence of a surface layer with a high diffusivity [4]. The high diffusivity in the N-implanted layers can be explained by the formation of amorphous or nanogained material. Recently it was shown that grain boundaries (GBs) in two- or multicomponent systems can contain a stable layer of a GB phase which is unstable in the bulk [18, 19]. The presence of such a GB layer can lead to an enhancement of the GB mobility [20], GB segregation [19, 21] and GB diffusivity [18]. In nanostructured materials up to 1/3 of all atoms can belong to the GB, and an increase of the diffusivity can be immense in comparison with coarse-grained materials. We can suppose that in the N-implanted stainless steel the layers of α -phase having higher diffusivity are present in GBs of the γ -matrix. Such layers can be responsible (a) for D_{eff} values which are higher than the D values for γ -Fe but lower than those for α -Fe and (b) for an activation energy Q which is close to the Q value for α -Fe.

The elevated temperature in the experiments [4] could lead to a dynamic relaxation of the defects generated during the implantation process. Therefore, in our experiments we studied the low-energy high-current N implantation without additional heating of the substrate, in order to reduce a possible dynamic relaxation of the defects. As a result, our data for D_{eff} in austenitic stainless steel are really higher than the extrapolation of the Arrhenius plot for the data taken from [4] (Fig. 3, thin solid line). The obtained D_{eff} value is very close to the D values for the bulk diffusion in α -Fe. On the other hand, the D_{eff} values obtained for ferritic (α) low-carbon steel are not much higher than those for austenitic (γ) stainless steel and practically coincide with the D values for α -Fe (Fig. 3). We

investigated also the influence of the implantation duration t that was not studied in [4] (Fig. 2). The resulting D_{eff} values reasonably coincide both for the ferritic and austenitic steels studied (Fig. 3). These facts support the hypothesis that the diffusion controls the enhanced N penetration during the low-energy high-current ion implantation into the stainless steel, and that this diffusion proceeds along the GB layers having a high diffusivity.

Acknowledgements

The financial support of the program for cooperation between Sweden and the former Soviet Union of the Royal Swedish Academy of Sciences, the German Federal Ministry for Education, Science, Research and Technology, the Alexander von Humboldt Foundation, joint program of Russian Foundation for basic Research and the Government of the Moscow district (contract 01-02-97039) and French embassy in Moscow is acknowledged.

References

- [1] S.J. Bull, A.M. Jones, A.R. McCabe, Surf. Coat. Technol. 83 (1996), p. 257.
- [2] Y. Jiraskova, C. Blawert, O. Schneeweiss, Phys. Stat. Sol. (a) 175 (1999), p. 537.
- [3] R. Günzel, M. Betzl, I. Alphonsa, B. Ganguly, P.I. John, S. Mukherjee, Surf. Coat. Technol. 112 (1999), p. 307.
- [4] D.L. Williamson, J.A. Davis, P.J. Wilbur, J.J. Vajo, R. Wei, J.N. Matossian, Nucl. Instr. Meth. B 127/128 (1997), p. 930.
- [5] S. Parascandola, R. Günzel, R. Grötschel, E. Richter, W. Möller, Nucl. Instrum. Meth. B 136–138 (1998), p. 1281.
- [6] N.V. Pleshivzev, A.A. Bazhin. "Physics of the Influence of Ionic Beams on Materials". Moscow, Vusovskaja Kniga Publishers, 1998, p. 32 (in Russian).
- [7] N. Vershinin, B. Straumal, K. Filonov, R. Dimitriou, W. Gust, M. Benmalek, Thin Solid Films 351 (1999), p. 190.
- [8] N. Vershinin, R. Dimitriou, M. Benmalek, B. Straumal, W. Gust, J. Vivas, J. Shulga, Surf. Coat. Techn. 125 (2000), p. 35.
- [9] H.R. Kaufman, J.M.E. Harper, J.J. Cuomo, J. Vac. Sci. Technol. 21 (1982), p. 764.
- [10] H.R. Kaufman, J. Vac. Sci. Technol. A 4 (1986) 764.
- [11] H.R. Kaufman, J.J. Cuomo, J.M.E. Harper, J. Vac. Sci. Technol. 21 (1982), p. 725.
- [12] H. Mehrer (ed.), Diffusion in Solid Metals and Alloys, Landolt–Börnstein New Series, Springer-Verlag, Berlin, III/26 (1990), p.496.
- [13] J. Hirvonen and A. Anttila, Appl. Phys. Lett. 46 (1985), p. 835.
- [14] T.V. Ischenko, S.V. Demishev and W. Gust, Comput. Mater. Sci. 17 (2000), p. 331.
- [15] S.V. Demishev, T.V. Ischenko, S.J. Blundell and J. Singleton, J. Phys. Cond. Mater. 9 (1997), p. 9199.
- [16] S.V. Demishev and T.V. Ischenko, Defect Diff. Forum, 143-147 (1997), p. 1535.
- [17] A.V. Byeli, O.V. Lobodaeva, S.K. Shykh and V.A. Kukareko, Nucl. Instr. Phys. B. 103 (1995), p. 533.
- [18] B. Straumal, E. Rabkin, W. Lojkowski, W. Gust and L. S. Shvindlerman, Acta Mater. 45 (1997), p. 1931.
- [19] L.-S. Chang, E. Rabkin, B. Straumal, P. Lejcek, S. Hofmann and W. Gust, Scripta Mater. 37 (1997), p. 729.
- [20] D.A. Molodov, U. Czubayko, G. Gottstein, L.S. Shvindlerman, B.B. Straumal and W. Gust, Phil. Mag. Lett. 72 (1995), p. 361.
- [21] B.B. Straumal, S.I. Prokofjev, L.-S. Chang, N.E. Sluchanko, B. Barezky and W. Gust, this issue, P1-226.